PERGAMON

Journal of Structural Geology 22 (2000) 489–503

JOURNAL OF STRUCTURAL GEOLOGY

www.elsevier.nl/locate/jstrugeo

Three-dimensional shape and emplacement of the Cardenchosa deformed pluton (Variscan Orogen, southwestern Iberian Massif)

J. Fernando Simancas*, Jesús Galindo-Zaldívar, Antonio Azor

Departamento de Geodinámica, Universidad de Granada, Campus de Fuentenueva, 18002 Granada, Spain

Received 28 June 1999; accepted 17 November 1999

Abstract

The Cardenchosa pluton is a Lower Carboniferous Variscan granite located in the southwestern Iberian Massif. It intruded along the contact between the Sierra Albarrana and Azuaga tectonic units. To the northwest the pluton connects with the left-lateral Azuaga fault. The pluton appears in the footwall of the low-angle normal Casa del Café fault, which crops out to the west of the granite. Gravimetric modelling shows the pluton to have a flat bottom at a depth of 2 km. Strain analysis of post-emplacement deformation of the pluton indicates that: (a) the deformation of the pluton accommodates the displacement of the Azuaga fault; and (b) the pluton prior to the solid state deformation was a lens-shaped laccolith of approximately 10 km diameter and 2 km thickness. The Cardenchosa pluton was a single pulse of magma trapped in a rheological discontinuity of the upper crust (the contact between the Sierra Albarrana and Azuaga units). The magma would ascend through dikes since no root has been detected. The tectonic scenario during the intrusion was one of regional extension.

1. Introduction

Ascent and emplacement of granitoids has received much attention in recent years with the advent of new theoretical developments and the application of geophysical methods for the 3D investigation of pluton geometry. Theoretical calculations have recently provided support for dike ascent of large volumes of magma through the continental crust (Clemens and Mawer, 1992; Petford et al., 1994; Petford, 1996). Dike ascent has been favoured in most recent papers at the expense of the hypothesis of diapiric ascent (Marsh, 1982; Weinberg and Podladchikov, 1995), although there remains much controversy on the issue (Paterson, 1994), especially concerning the viability of magma segregation from the source through dikes (Weinberg, 1999). Claims for both mechanisms during the same ascent have been defended in the literature: diapiric ascent in the hot lower crust and diking in the upper crust (Weinberg, 1996). Regarding the final emplacement of the magmas in the upper crust, 3D shapes (e.g. McCaffrey and Petford, 1997) and strain in pluton aureoles (e.g. Paterson and Vernon, 1995) are key issues to be addressed. This discussion has been traditionally limited by the failure of classical structural studies to establish the shape of the plutons accurately (but there are conspicuous exceptions, e.g. Rosenberg et al., 1995). The combination of surface geological observations with geophysical techniques—notably, gravimetric surveys (Bott and Smithson, 1967; Vigneresse, 1990; Ameglio et al., 1997) and, to a lesser degree, the mapping of the anisotropy of magnetic susceptibility (Guillet et al., 1983; Bouchez, 1997), play a crucial role in deepening our knowledge of 3D pluton shapes. These studies commonly show that pluton shapes are tabular (Brisbin and Green, 1980; Guineberteau et al., 1989; Román-Berdiel et al., 1995b; Aranguren et al., 1996, 1997; McCaffrey and Petford, 1997), although voluminous roots have also been imaged (Guineberteau et al., 1987; Dehls et al., 1998).

* Corresponding author.
E-mail address: simancas@goliat.ugr.es (J.F. Simancas).

0191-8141/00/$ - see front matter
PII: S0191-8141(99)00178-9

On the other hand, analogue modelling suggests that subhorizontal rheological boundaries can in some cases determine the trapping and accumulation of magma as tabular plutons (Román-Berdiel et al., 1995a, 1997). There are also proposed examples of accumulation of magma in low stress zones along fault systems (e.g. Guineberteau et al., 1987; Hutton, 1988; Tikoff and Teyssier, 1992; Grocott et al., 1994), although the compatibility between rates of tectonic processes and pluton filling has been debated (Paterson and Fowler, 1993a; Hanson and Glazner, 1995). All this new geometrical and experimental information has consequences for the much-discussed room problem issue, because the growing of tabular bodies (Pollard and Johnson, 1973; Corry, 1988; Román-Berdiel et al., 1995a; Kerr and Pollard, 1998; Cruden, 1998) or the magmatic accumulation in low stress zones can take place with little deformation of the host rocks. On the contrary, diapiric emplacement (England, 1992) or in situ inflation of plutons (Ramsay, 1989; Molyneux and Hutton, 1995) should imply important deformation of the host rocks. Finally, for some authors, emplacement is best viewed as the combined action of multiple mechanisms among which stoping would play an important role (Paterson and Fowler, 1993b; Paterson et al., 1996). In this varied and controversial background, we claim that pluton shape is one of the basic features that can reflect the dominant emplacement mechanism. Consequently, the availability of a catalogue of 3D geometries of differently sized plutonic bodies is a basic condition for a fruitful discussion of the problem of emplacement (and ascent) of magmas in the upper crust.

This work contributes to the understanding of epizonal pluton emplacement by demonstrating the tabular 3D geometry of the Cardenchosa pluton, a Variscan intrusive located in the southwestern Iberian Massif. We have performed a structural and gravimetric study that has given us the present shape of this pluton and, as this image is strongly influenced by solid state deformation, we have approximately restored the pluton to its original (intrusive) shape.

2. Geological setting

The Cardenchosa pluton is exposed to the south of one of the suture contacts of the Variscan Orogen in

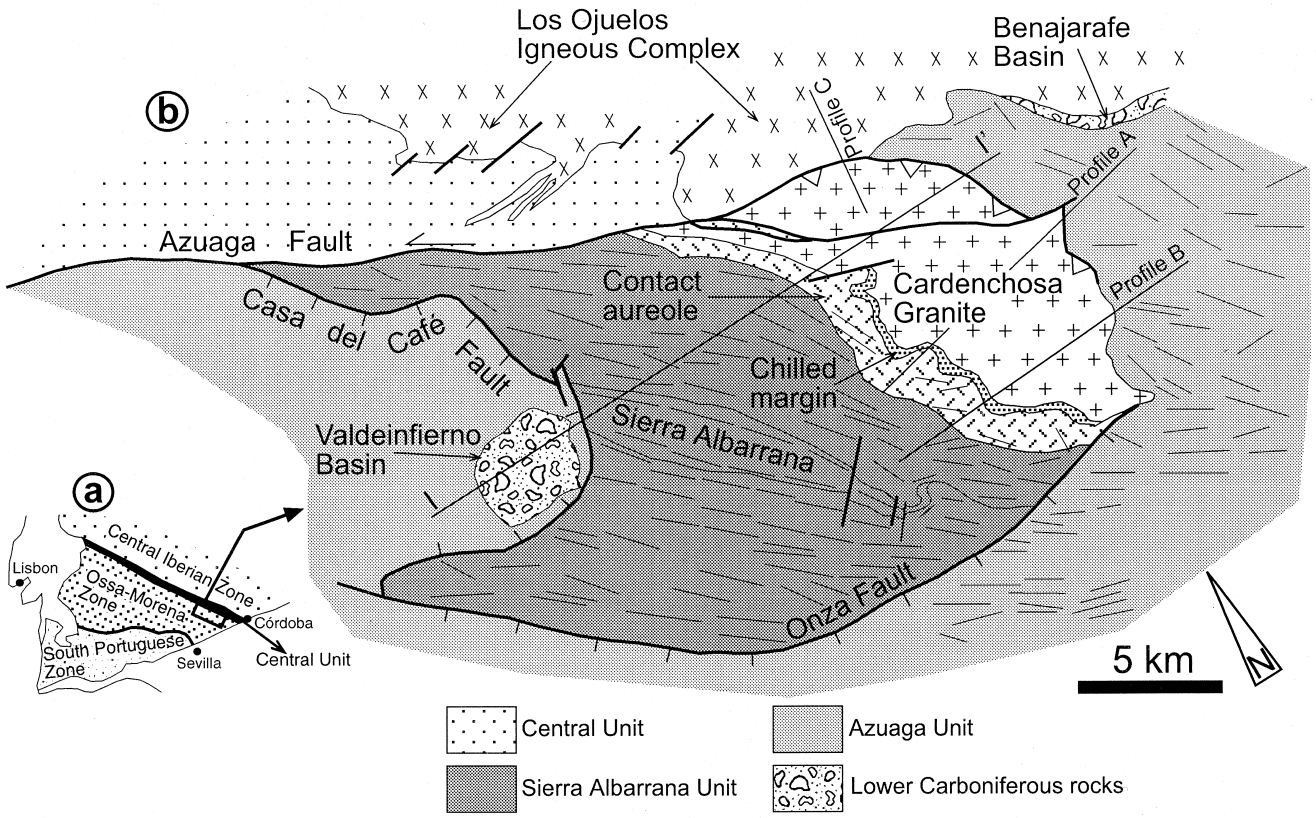

Fig. 1. (a) Main tectonic zones in the SW Iberian Massif, and location of the Cardenchosa pluton. (b) Geology around the Cardenchosa pluton. Note the termination of the Azuaga strike-slip fault, and the Lower Carboniferous basin—Valdeinfierno Basin—on the hanging wall of the low-angle normal Casa del Café fault. Note also that the Cardenchosa pluton has intruded in between the Sierra Albarrana and Azuaga units. Short thin lines represent the orientation of the regional schistosity in the country rocks of the Cardenchosa pluton. A, B and C: gravity and magnetic anomaly profiles shown in Fig. 6. I–I′: cross-section in Fig. 11(a).

the Iberian Massif, the boundary between the Ossa-Morena and the Central Iberian zones (Fig. 1a). This suture, called the Central Unit, is marked by a strongly deformed and metamorphosed, NW–SE-trending band made up of metasediments, orthogneisses and amphibolites (Azor et al., 1994). To the SE, the suture rocks are cross-cut by a Lower Carboniferous volcanic–plutonic, acid–basic igneous complex (Los Ojuelos igneous complex, Delgado Quesada et al., 1985; Fig. 1b), which includes the Cardenchosa pluton. At present, the Central Unit is separated from the northern border of the Ossa-Morena Zone by subvertical left-lateral strike-slip faults (e.g. the Azuaga Fault, Fig. 1b). These faults are part of a linked left-lateral, strike-slip fault system that affects the whole southwestern Iberian Massif in a late stage of the Variscan orogenesis (Simancas, 1983; Sanderson et al., 1991; Jackson and Sanderson, 1992).

The Cardenchosa Pluton is located at the boundary between two tectonic units, namely, the Sierra Albarrana (in a lower position) and Azuaga units (Azor, 1994, Fig. 1b). The Sierra Albarrana unit is made up of Lower Palaeozoic metasedimentary rocks intensely deformed by folding and ductile shearing and affected by low- to high-grade, low-pressure metamorphism (Azor et al., 1994; Azor and Ballèvre, 1997). Deformation and metamorphism are coeval, with an age between 390 and 350 Ma according to $^{40}Ar/^{39}Ar$ radiometric datings (Dallmeyer and Quesada, 1992). In the area near the Cardenchosa pluton, the Azuaga unit consists of Middle Cambrian siliciclastic rocks affected by syn-schistose upright folding and very low- to low-grade metamorphism. The actual boundaries between both units are faults downthrowing the Azuaga unit (Fig. 1b): to the west, the low-angle normal Casa del Café fault, responsible for the formation of the Upper Tournaisian Valdeinfierno basin; to the south, the high-angle Onza fault, with components of normal and left-lateral displacement. To the north, the left-lateral Azuaga fault separates the Sierra Albarrana unit from the Central Unit.

3. The Cardenchosa pluton

The Cardenchosa pluton is made up of two granitic facies. The more abundant facies is a coarse-grained, slightly porphyritic granite with up to 4 cm feldspar phenocrysts. A second minor facies, restricted to the western border of the pluton, is a chilled margin (Fig. 1b) made up of medium to fine-grained leucocratic alkaline granite. A petrographic description and some chemical analyses of this granitic pluton have been provided by Garrote and Sánchez Carretero (1979). Enclaves are scarce in the pluton, the vast majority of them being microgranular, of a likely igneous derivation and an original basic composition. Other enclaves are xenoliths from the country rocks, and a few mappable outcrops of schist surrounded by granite are interpreted as roof pendants (Fig. 2). Inside the Cardenchosa pluton there are a suite of ENE–WSW-trending mineralized fluorite–barite veins and a NW–SE-trending diabase–rhyolite dike swarm intruding the northern part of the pluton and the adjacent country rocks (Fig. 2). The homogeneous composition of the pluton and its limited map extent (about 60 km^2) suggest that it originated by a single pulse of magma (Pitcher, 1979).

The country rocks of the Cardenchosa pluton are as follows: (1) along the western border, medium-grade micaschists belonging to the Sierra Albarrana unit; (2) along the eastern and southern borders, slates with some quartzite intercalations belonging to the Azuaga unit; and (3) along the northern border, basic igneous rocks belonging to Los Ojuelos igneous complex (Fig. 1b). The metamorphic contact aureole associated with the pluton is well developed along the western and southern margins, where it consists of a 1–2-km-wide band of hornfelses (Garrote, 1976; Azor and Ballèvre, 1997). The eastern margin of the pluton is affected by a high-angle reverse fault that hides the metamorphic contact aureole (Fig. 1b). The highest-grade metamorphic assemblages recorded by the hornfelses in the contact aureole are represented by the appearance of andalusite, biotite, fibrolitic sillimanite, garnet and K-feldspar just at the contact with the pluton. In the external aureole, contact assemblages are made up of andalusite, biotite and garnet. The microtextures shown by garnet and andalusite porphyroblasts indicate a static growth over a previous regional foliation. According to these assemblages, especially the coexistence of andalusite and K-feldspar in the innermost part of the aureole, maximum pressures of no more than 2 kbar and temperatures between 500 and 600°C can be estimated for the contact aureole. Consequently, the Cardenchosa pluton can be considered to have intruded in the upper crust at a maximum depth of 5–6 km.

The age of the Cardenchosa pluton cannot be established accurately since no radiometric ages are available. However, the pluton is most probably of Lower Carboniferous age since it appears to be related to the Los Ojuelos igneous complex, which includes volcanic rocks interlayered with sedimentary Lower Carboniferous rocks (Delgado Quesada et al., 1985). Moreover, the contact metamorphism obliterates the regional foliation in the Sierra Albarrana unit, which is Devonian in age (Dallmeyer and Quesada, 1992; Azor and Ballèvre, 1997).

4. Structural features

The Cardenchosa pluton is an elongate, subconcordant body striking NNW–SSE, with a tail at its northwestern part that joins the left-lateral, strike-slip Azuaga Fault (Figs. 1b and 2). The eastern border of the pluton is a west-dipping, high-angle reverse fault with decreasing displacement to the south. The fault zone consists of some breccias and kink folds in country rocks, which indicate the upwards movement of the pluton over the country rocks. The southern and western borders of the pluton are only affected by minor left-lateral, strike-slip faults, the contact showing dips towards the pluton or towards the country rocks (Fig. 2).

The fabric of the pluton is characterized by a foliation trending generally NNW–SSE, parallel to the longest dimension of the pluton (Fig. 2). The dips of the foliation are generally steep, but they present some variation defining an open folding. At outcrop scale, the foliation is defined by a preferred orientation of K-feldspar phenocrysts (often broken) and elongate quartz grains (Figs. 3 and 4). Microscopically, the quartz appears as aggregates of small grains resulting from recrystallization and grain growth (Fig. 4c). The foliation features a strong development in the north-

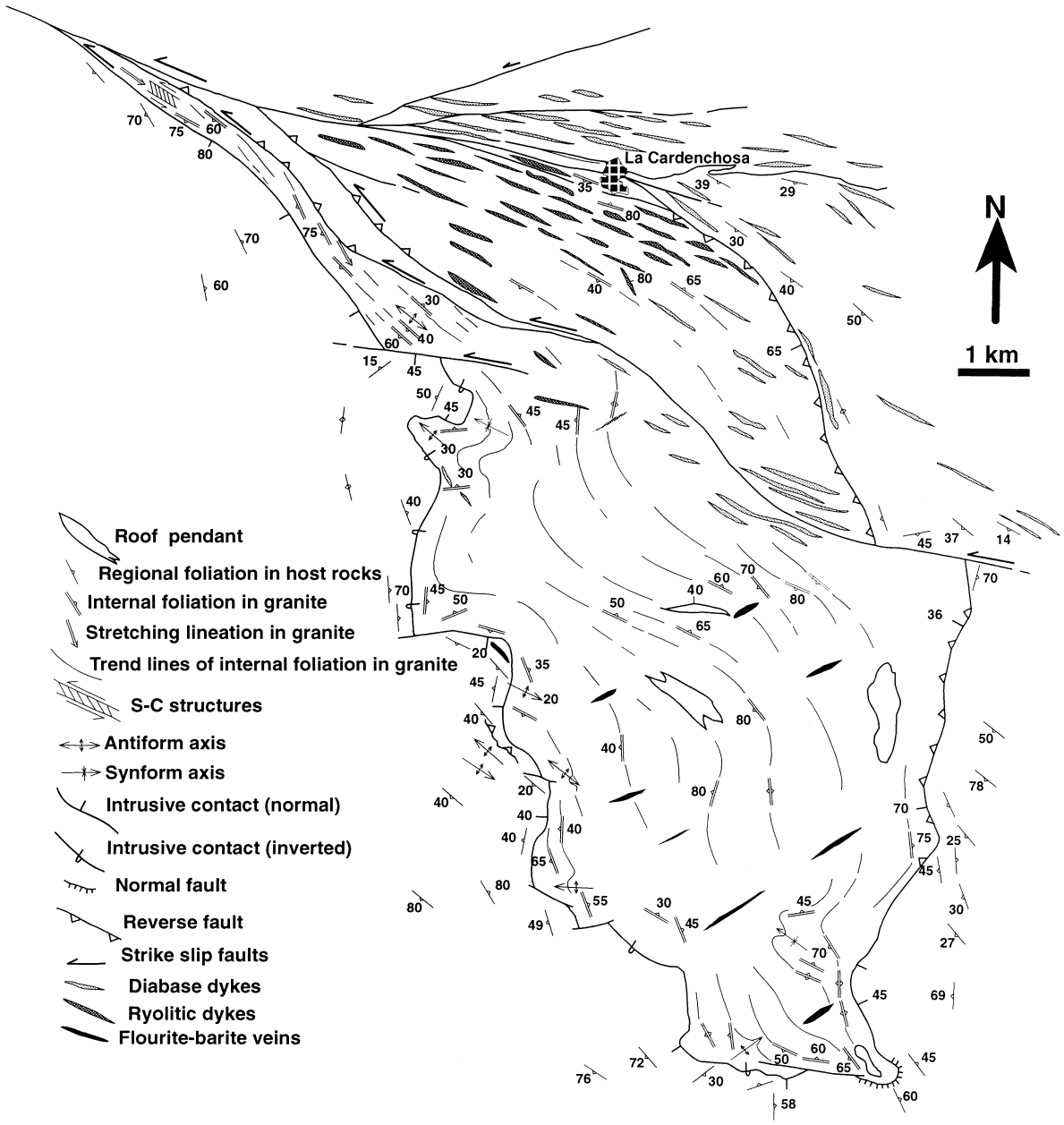

Fig. 2. Structural map of the Cardenchosa pluton.

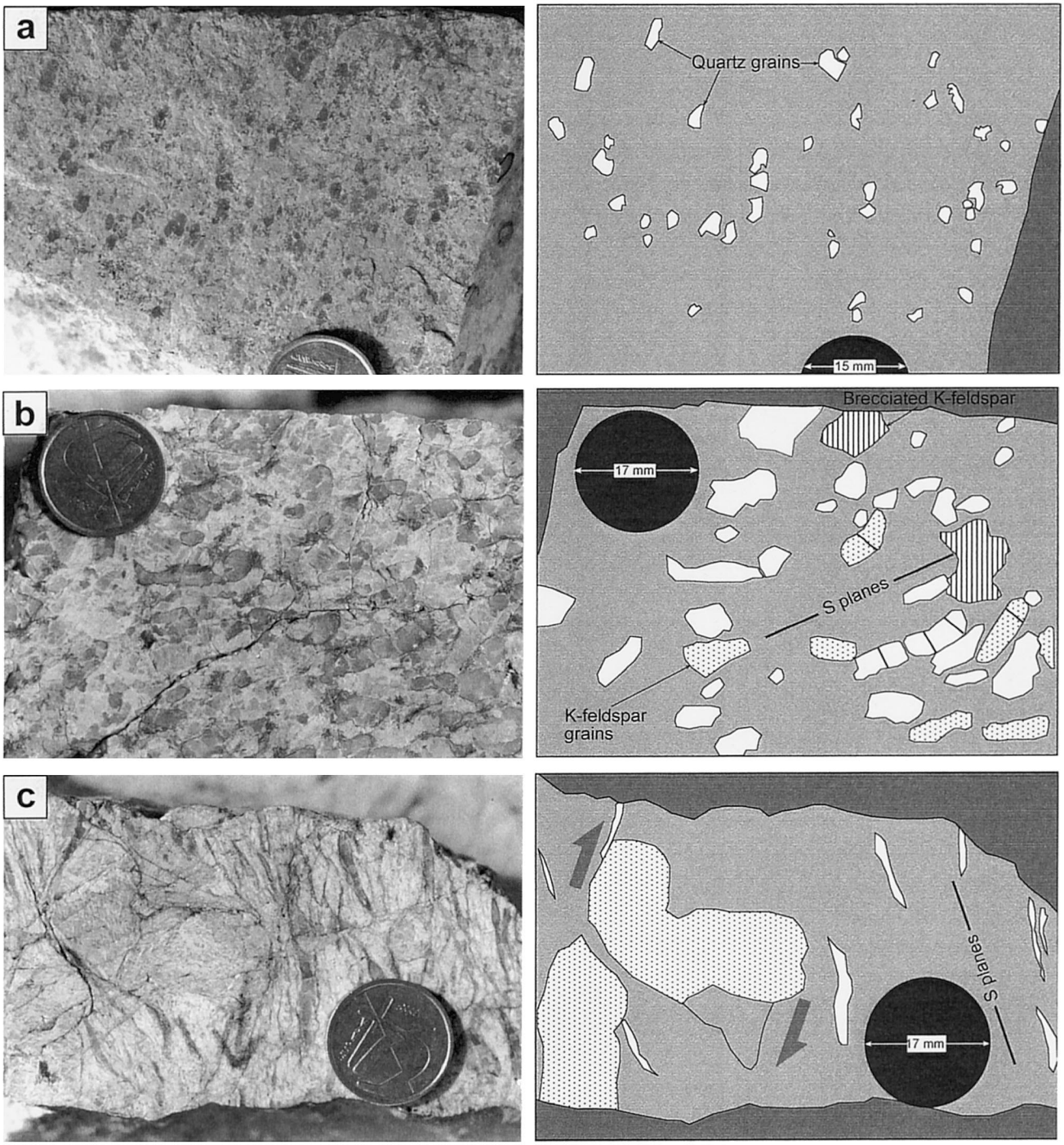

Fig. 3. Evolution of the shape of quartz grains as strain increases. (a) Very low-strained medium-grained granite (left) from which the contours of some quartz grains are represented in the sketch located to the right. Note the very low axial ratios of quartz grains. The white ground in the photograph (left) is a mass of K-feldspar grains. (b) Medium-strained coarse-grained granite. Note the higher axial ratios of quartz grains, some of them showing fractures perpendicular to the longest dimension. Fracturing is much more common in K-feldspar grains, which frequently appear brecciated. All these features are represented schematically on the right side, where some grains have been depicted (white pattern: quartz grains; dotted pattern: K-feldspar grains; ruled pattern: brecciated K-feldspars). (c) High-strained coarse-grained granite. A large K-feldspar porphyroclast is broken and distorted to accommodate shortening, and develops an albitic strain shadow. Quartz grains show very high axial ratios.

west part (the tail) of the pluton (Fig. 3c). Here, quartz appears as ribbons of recrystallized new grains (Fig. 4d), feldspars are usually broken (Figs. 3b and 4e) but also show albite recrystallization (Figs. 3c and 4f), and a few grains of orthoclase have small myrmekites along borders parallel to the foliation (Fig. 4f). There is microstructural evidence for plastic deformation of quartz in the form of subgrain boundaries (Fig. 4d). The orientations of feldspars (poles to [010]) and micas (poles to [001]) in samples of medium-grained high-strained granite, measured under the microscope, are shown in Fig. 5(a).

The fabric of the pluton is generally planar but in the tail a stretching lineation is defined by quartz rib-

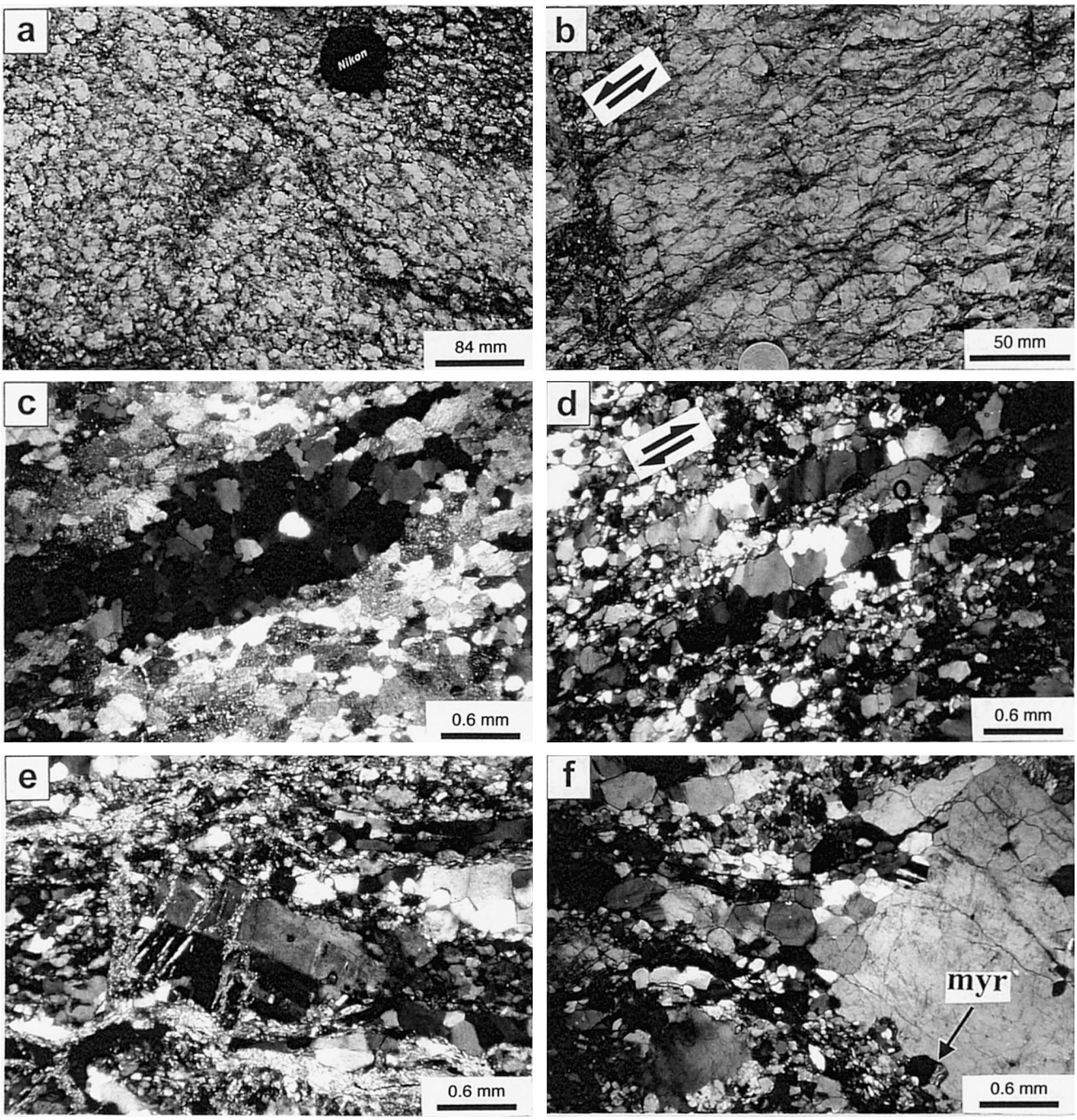

Fig. 4. (a, b) Structural features of the Cardenchosa granite: (a) low deformed granite, (b) intensely deformed granite. Arrows indicate the sense of shearing as deduced from *S*/*C* structures. (c–f) Photomicrographs of highly deformed granite: (c) ellipsoidal quartz domain; (d) quartz micrograins showing subgrain boundaries oblique to the foliation defined by quartz ribbons, arrows indicating the sense of shearing inferred; (e) broken K-feldspar porphyroclast; (f) K-feldspar porphyroclast with myrmekite in the shortening quarter and a tail made up of recrystallized grains of quartz and albite.

bons. The lineation strikes NW–SE and plunges gently to the SE (Fig. 2). Associated with the planar–linear fabric in the tail of the pluton there are *S*/*C* and other asymmetrical structures indicating a non-coaxial flow with a left-lateral sense of movement (Figs. 3c and 4b). Other kinematic microscopic criteria, such as quartz subgrain boundaries oblique to the foliation, confirm the same kinematics (Fig. 4d). Quartz *c*-axis preferred orientation has been investigated in medium- to fine-grained strongly deformed samples of the northwestern border. The diagrams obtained (Fig. 5b) show asymmetric single girdles which suggest temperatures in the range 300–600°C (Gapais, 1989; Okudaira et al., 1995). The asymmetry of the girdles is also consistent with a left-lateral sense of movement.

Structural studies of igneous bodies always raise the question of the magmatic or tectonic solid-state flow origin of the foliation (e.g. Paterson et al., 1989). As

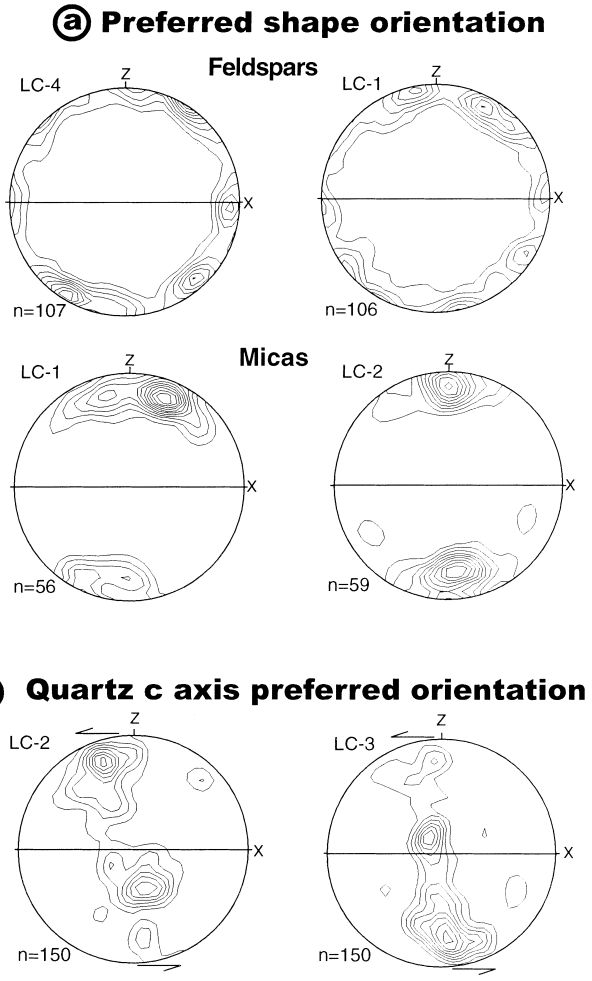

Fig. 5. (a) Preferred shape orientation of feldspars [poles to (010)] and micas [poles to (001)]. (b) Quartz *c*-axis fabrics; arrows indicate the sense of shearing inferred. All samples—LC1 to LC4—correspond to intensely deformed granite. Lower-hemisphere equal-area projection; contours at 1%. X: stretching lineation.

for the Cardenchosa pluton, several arguments strongly support a solid-state flow origin for the foliation, i.e. a post-emplacement deformation. First of all, quartz grains are flattened and show subgrain microstructures (Fig. 4d). Moreover, K-feldspar phenocrysts are usually broken and stretched (Figs. 3 and 4). Furthermore, quartz *c*-axis preferred orientation indicates deformation under middle- or low-temperature conditions. Finally, the strong development of the foliation in the tail of the pluton, where it coincides with an important fault (Fig. 2), strongly suggests a relationship between pluton deformation and faulting.

A distinctive strain aureole is not well developed; a foliation in the country rocks attributable to the pluton emplacement is lacking. This fact does not mean that there is zero deformation in the country rocks due to the intrusion or related to the solid-state deformation of the pluton. The intense regional schistosity previously developed in the country rocks, probably accommodated some additional shortening without the formation of a new penetrative foliation. The regional schistosity accommodates itself around the pluton (Figs. 1b and 2) and is deflected around the southern border of the pluton bearing witness to some flattening attributable to the emplacement and/or the post-emplacement solid-state deformation. There are, in the country rocks, kink folds and minor reverse faults, which can be correlated with the shortening structures observed in the pluton.

5. Gravimetry and magnetometry

Few geophysical data are available for this area and consist only of the 1:1 000 000 aeromagnetic anomaly map and the 1:500 000 Bouguer anomaly map of the Spanish Instituto Geográfico Nacional. In order to have enough data to determine the main features of the deep structure of the granite body studied, we have measured complementary gravity and magnetic data in the area.

The 1:500 000 Bouguer anomaly map (without topographic correction) shows that the region of study is located in an area characterized by positive (0–25 mGal) low-gradient anomalies. The anomaly trend is not well defined, but two main trends (NE–SW and NW–SE) can be recognized. These trends are parallel to the NE–SW elongate anomalies related to the Guadalquivir Basin and Betic Cordillera to the south, and the NW–SE Variscan structures to the northeast, respectively. The map is not accurate enough to reveal any anomaly related to the granite body. By contrast, the 1:1 000 000 aeromagnetic anomaly map shows that a NNW–SSE elongate minimum, with values of 0 nT or slightly negative (up to −20 nT) corresponds to the pluton. This minimum is bounded to the east and to

the west by well-defined ENE–WSW elongate dipoles of more than 150 nT of difference between maxima and minima. These dipoles are parallel to the major Variscan structures of the area.

We have acquired complementary gravimetric and magnetic measurements along two E–W profiles across the pluton and a complementary N–S profile along its northern boundary, marked as A, B, and C in Fig. 1(b). The gravity measurements have been done with a Worden gravimeter, with temperature compensation and maximum precision of 0.01 mGal. A GEM neutron precession magnetometer, with an accuracy of 1 nT has been used to determine the total magnetic field intensity. Measurement points have been positioned by GPS and a barometric altimeter, which has a maximum precision of 0.5 m in altitude. Measurements have been done with a mean spacing of 150 m along profiles.

Measurements have been done in cycles of less than three hours in order to make a linear correction of gravimeter and altimeter drifts. Altimetric data have been taken in the base station from the topographic map and, after drift correction, have been estimated for each measurement station. We have calibrated our gravimetric data with the absolute gravity measurements of the base station of the Instituto Geográfico Nacional located in Córdoba. Gravity measurement in each field station has made it possible to calculate the Bouguer anomaly. We have considered a standard density (2.67 g/cm^3) for Bouguer correction. However, we have not considered the terrain correction, taking into account that for this area it is low with respect to the anomalies studied. Magnetic data have been corrected in each cycle for diurnal variations, and the IGRF95 has been subtracted in order to determine the total field magnetic anomalies.

The Bouguer and total field magnetic anomalies determined in our study are of the same range of values as those of the general maps of the Instituto Geográfico Nacional. Magnetic anomalies (Fig. 6) are located only in the northern and eastern pluton borders, being related to the dikes of basic igneous rocks (Fig. 2). The absence of significant magnetic anomalies in the area cropping out of the pluton confirms its homogeneous acid character, which is also borne out by field data. In the profiles A and B, orthogonal to the pluton elongation, the values of regional gravity anomaly decrease eastwards (Fig. 6). The slope in the southern (B) profile is higher than in the northern one (A), probably due to the influence of other bodies located to the southwest of our study area. Profile A

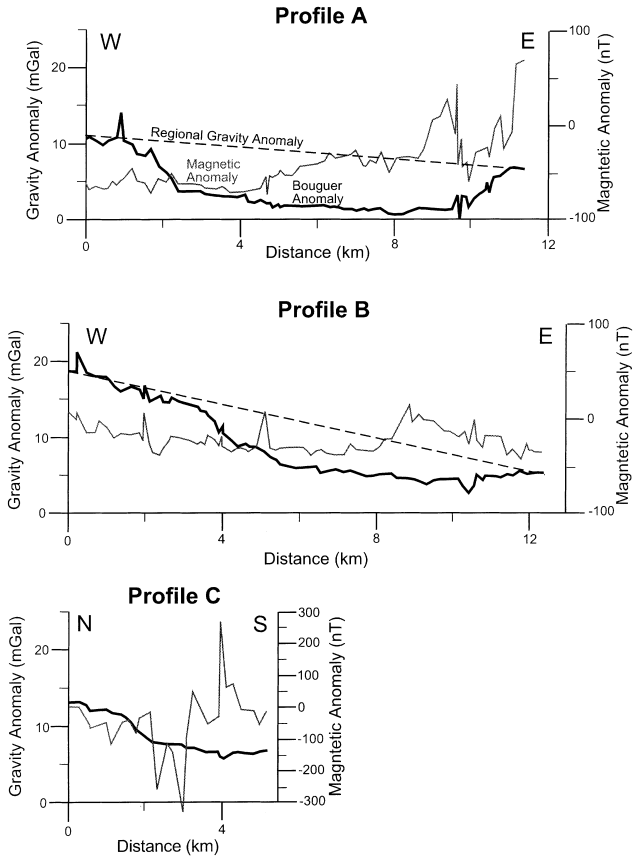

Fig. 6. Gravity and magnetic anomaly profiles. For location, see Fig. 1(b).

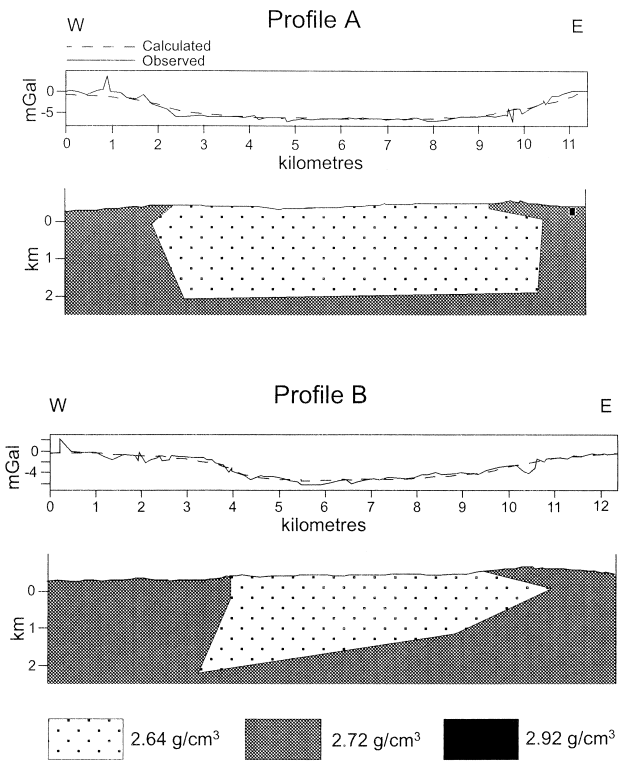

Fig. 7. Residual gravity anomaly models of the Cardenchosa pluton, according to the gravity anomalies in profiles A and B of Fig. 6. The 2.64 g/cm^3 body corresponds to the modelled pluton shape. See text for further explanation.

has a better shape than profile B, establishing the residual anomaly by profile smoothing. In both profiles, residual anomaly corresponds to a minimum of about 7–8 mGal, and this minimum has a clear flat bottom in profile A (Figs. 6 and 7), thus suggesting an approximate horizontal slab geometry for the granite body.

Two-dimensional models of residual gravity anomaly have been developed along the two E–W oriented profiles in order to determine the main geometrical features of the granite body in depth. Both profiles (A and B in Fig. 1b) are located far from the north and south pluton borders, the anomalous body being presumably two-dimensional. We have considered in the models the densities determined by Campos and Plata (1991) in extensive sample studies of other bodies located to the northwest of the pluton studied. These authors establish that the mean density of the slates in the area is 2.72 g/cm^3, which is considered in our models as representative of the country rocks. In addition, they determined that the mean density of acid granites is 2.64 g/cm^3, a value that we have assumed for the granite body studied here. We have included a body at the eastern end of profile A, of density 2.92 g/cm^3, which could represent the basic dikes that largely outcrop in this sector. An additional geometrical constraint considered in developing the models is the position and orientation of the pluton boundaries determined by field observations.

Both gravity anomaly models indicate that the granite body is shallow, with a maximum depth comprised between 1 and 2 km (Fig. 7). A slight variation in densities does not modify significantly the determined depths. The bottom may be nearly flat, subhorizontal

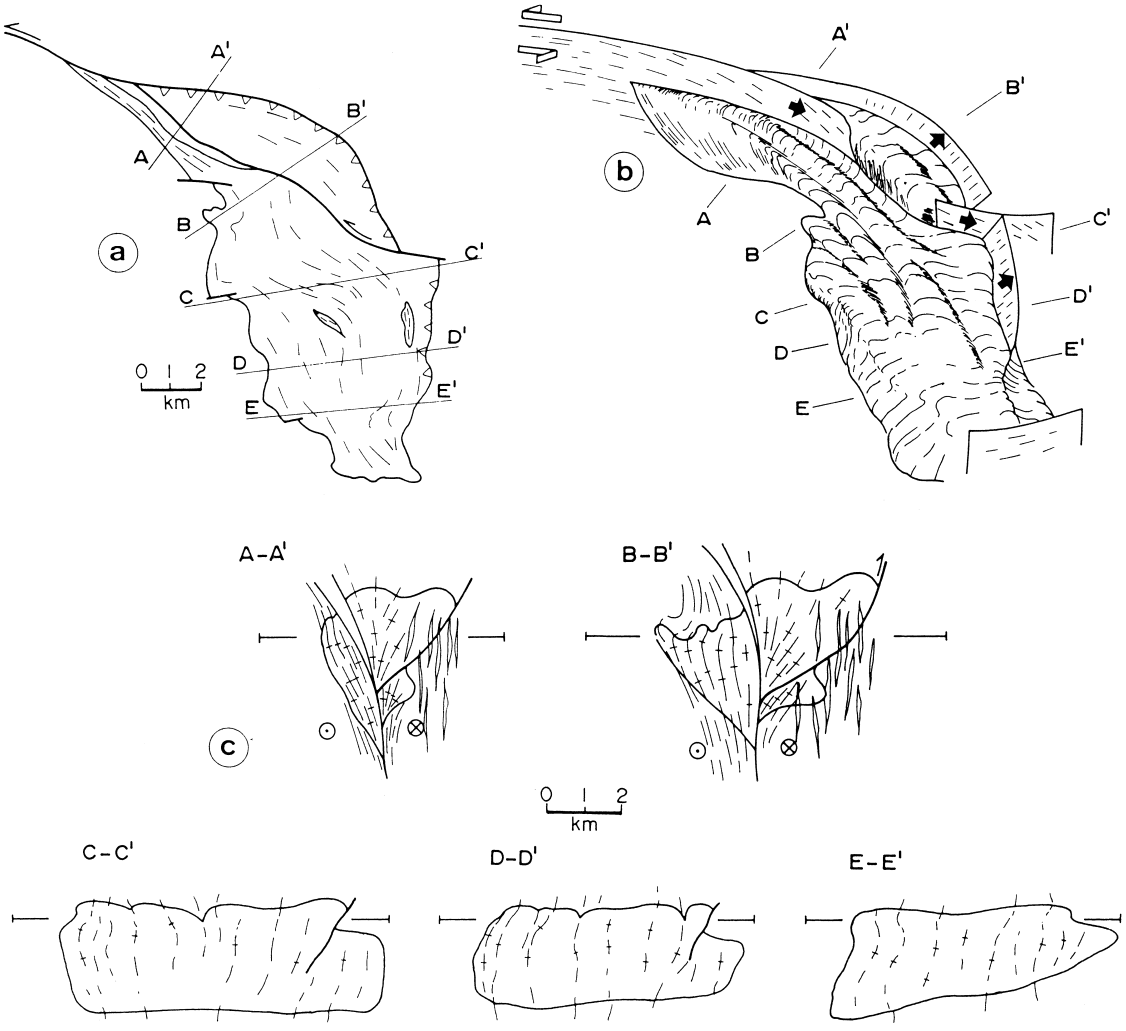

Fig. 8. Shape of the Cardenchosa pluton as inferred from combined geological and gravimetric data. (a) Sketch map of the pluton with the location of cross-sections. (b) Schematic 3D view of the pluton also showing the location of the cross-sections. (c) Geological cross-sections from the northwestern tail (AA′) to the southern part (EE′) of the Cardenchosa pluton.

in profile A, or slightly dipping to the west in profile B. In both profiles, the body enlarges with depth, a feature especially relevant in the eastern side of profile A, where the surface boundary is vertical due to a fault, but the body extends in depth towards the east (Fig. 7).

6. Three-dimensional shape and strain

Geological mapping provides data for the geometry of the pluton near the surface, but leaves the deep structure unconstrained. Gravity data have shown that the pluton has a flat bottom at a depth of approximately two kilometres. Combining both kinds of data, it has been possible to construct well-constrained serial cross-sections of the Cardenchosa pluton (Fig. 8). The resulting 3D shape (Fig. 8b) is a tabular body with average dimensions 12 km (length) × 5 km (width) × 2.5 km (thickness). This value of thickness reflects our inference that erosion has not removed an important volume of the pluton, as supported by (a) the leucocratic chilled margin in the western and southern borders, (b) the moderate outward dips of the external contact in many places, (c) the existence of few roof-pendants, and (d) the depth enlargement deduced from the gravity models. The northern part of the granite presents a more complex geometry than the southern one, this being obviously related to differences in the solid-state deformation undergone by the pluton. As a result of this post-emplacement deformation, the shape of the pluton has been modified since intrusion.

A strain analysis has been performed in order to restore approximately the Cardenchosa pluton to its original intrusive shape. The strain marker that has mainly been used is the macroscopic shape of quartz grains. The harmonic mean (Lisle, 1977) and sometimes also the R_f/ϕ method (Ramsay, 1967) have been applied to these markers in order to compute strain. It is not important whether or not the quartz grains (at present aggregates of recrystallized micrograins) were always single crystals before deformation, and only the reasonable assumption that they were on average equidimensional needs to be considered. This assumption is supported by the variation of quartz grain shapes from nearly equidimensional in low deformed granite to very elongate in highly deformed granite (Fig. 3). However, when the quartz forms ribbons it is not suitable for that purpose, and in such cases the distribution of centres of feldspar phenocrysts (Fry method—Fry, 1979) has been used as strain markers. As a whole, 28 strain determinations have been made in 17 different outcrops (Fig. 9).

The orientation of the principal axes of strain

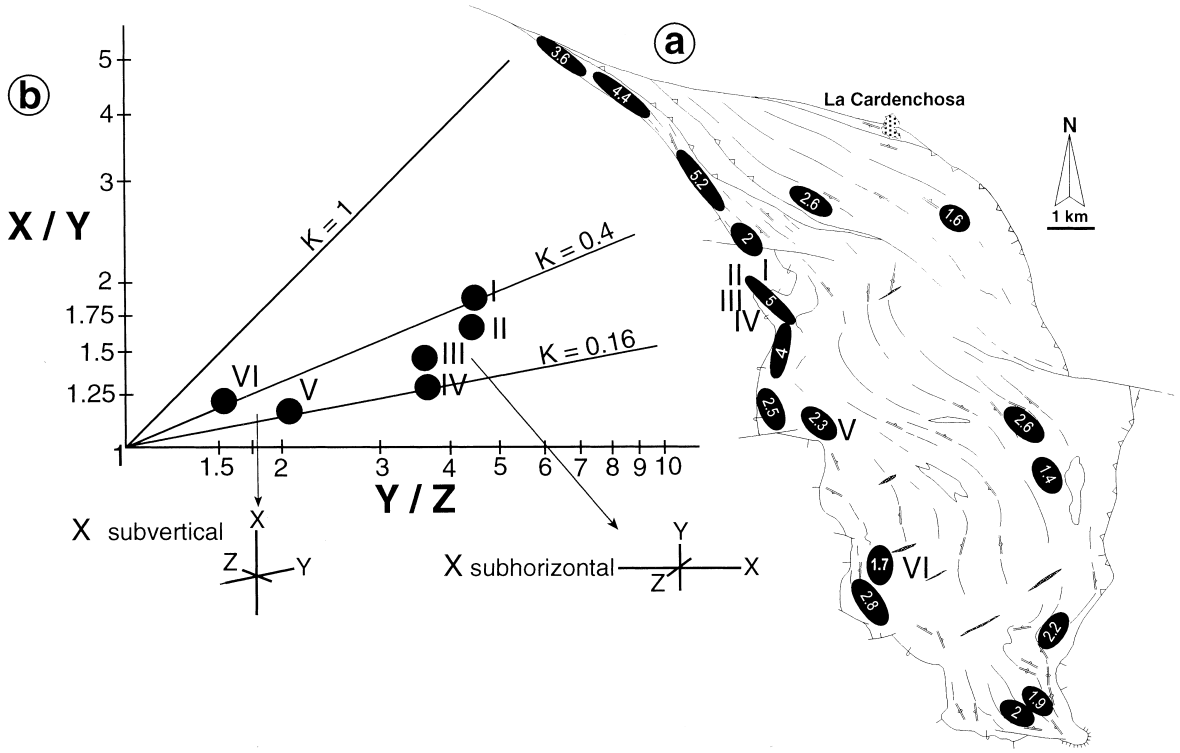

Fig. 9. (a) Strain map showing strain ellipses on subhorizontal surfaces. See text for further discussion. (b) Flinn diagram with the plots of the strain ellipsoids I–VI whose location is indicated in the strain map. Note that ellipsoids I, II, III and IV have a different orientation than ellipsoids V and VI.

(X, Y, Z) is not constant all over the pluton. In the northwest part, a clearly defined stretching lineation indicates that the X-axis is subhorizontal and trends NW–SE. In the remainder of the pluton, no stretching lineation can be observed but sometimes a faint preferred orientation of the long axis of quartz grains is detected in the foliation plane. Such a faint orientation is steep, which means that, contrary to the northwest part, the X-axis is subvertical and not markedly different from the Y-axis in the major part of the pluton (central and southern parts).

The main results of the strain analysis are presented in Fig. 9, where the ellipses on the map (Fig. 9a) are strain ellipses perpendicular to the foliation and contained in subhorizontal outcropping surfaces, i.e. XZ sections in the tail and sections near YZ (but very similar to XZ because $X \approx Y$) in the remainder of the pluton. In a few cases it has been possible to calculate strain ellipsoids from the three mutually perpendicular principal sections, the ellipsoids being of $K < 1$ value (Fig. 9b). The strain data and the geological mapping clearly depict three domains of deformation (Figs. 9a and 8b): (a) the southern half of the pluton, characterized by a moderate strain that is reflected in a poorly to moderately defined foliation without any noticeable lineation; (b) the northern part of lensoid shape, bounded by faults, with strain and fabric similar to those of the southern part; and (c) the tail-shaped northwestern border, more intensely strained and showing a well-developed planar–linear fabric with subhorizontal stretching lineation. The ellipsoids in two localities of the southern part, labelled V and VI in Fig. 9(a, b), are probably representative of the strain in the southern domain. Assuming no volume change, they suggest a modest stretching of 30–45% along X (steeply plunging), stretching of only 10–20% along Y (approximately subhorizontal and striking NNW–SSE) and shortening of 30–45% along Z (subhorizontal and striking ENE–WSW). The small stretching in the NNW–SSE direction is confirmed by the existence of a few ENE–WSW extension veins along the pluton, filled in with fluorite and barite (Fig. 2). The ellipsoids labelled I, II, III, and IV (Fig. 9a, b) come from the same location (a little quarry). They indicate a more intense stretching along X (100–150%; subhorizontal and striking NW–SE) and along Y (35–40%; subvertical), with 65–70% of shortening in the Z direction (striking NE–SW). This latter computed strain seems to apply only to a restricted area because it is located in a sector of complex deformation between the southern low-strain domain and the northwestern high-strain tail (Figs. 9a and 8b). No strain ellipsoid has been computed in the tail itself, although it is here where an intense planar–linear fabric with strong subhorizontal, NW–SE stretching lineation can be observed. Consequently, high strain ellipsoids of $K \approx 1$ should be expected in the tail.

The characteristic shape of the pluton (a tail in its northwestern part which connects with the Azuaga left-lateral strike-slip fault), together with the kinematic data (left-lateral shear sense in the tail, as deduced from S/C structures, subgrain boundaries and quartz c-axis preferred orientation) and the strain data available lead us to propose a simple two-dimensional model which approximately accounts for the pluton deformation. In this model, deformation is factorized into a pure shear component followed by a simple shear one (Fig. 10a). The pure shear is considered homogeneous all over the pluton and its deformation matrix has been established from the mean changes of length computed from the strain ellipsoids in the southern part of the pluton: 40% of E–W shortening and 15% of N–S stretching. The simple shear is clearly heterogeneous, increasing from south to north. From the resulting general deformation matrix (Fig. 10a), calculations (Ramsay and Huber, 1983, equations B.14 and B.19) provide values of the shear strain (γ) which approximately fit strain ratios and ellipse orientations on the map section (Fig. 10a, b). A sector whose strain is markedly different from the one predicted by the model is the northern part of lensoid shape bounded by two faults with reverse and left-lateral components of slip. As shown in the cross-sections (Fig. 8c) and in the block diagram (Fig. 8b), this area is a wedge of the pluton pushed to the NW and extruded upward. In this area, the granitic body has probably behaved in a different way in order to accomplish the displacements prescribed in the general displacement field, i.e. instead of deforming entirely in a ductile manner it has accommodated one part of the displacements by brittle oblique extrusion and the other part by ductile strain. Strain compatibility requires deformation in the country rocks. As previously stated, no distinctive strain aureole has been found, but regional foliation is deflected around the pluton (Fig. 1b), implying that strain in the country rocks is accommodated by the pre-intrusion regional foliation.

The simple model of deformation for the Cardenchosa pluton, in addition to providing a rough picture of the displacement field, can be used in two different ways. On the one hand, it serves to explain the sudden disappearance of the regionally important left-lateral strike-slip Azuaga fault (Fig. 1b). In this respect, it is clear that the displacement due to the simple shear component in the tail of the pluton (about 12 km; Fig. 10b) plus the displacement due to the shortening by pure shear (about 4 km) account for the greater part of the estimated strike displacement ($\sim$20 km) of the Azuaga fault, i.e. the strike displacement of the fault is accommodated by the deformation observed in the pluton (Simancas et al., 1997). On the other hand, the

model enables us to restore approximately the shape that the pluton had before its post-intrusion deformation. Unfortunately, the accuracy of the model is not sufficient to perform a detailed restoration, but from Fig. 10(b), the image of a more or less equidimensional intrusion as seen in plan is obvious. Instead of the square shape shown schematically in Fig. 10(b), a rounded shape (Fig. 10c) is geologically more plausible. As for its thickness, it is at present about 2.5 km, but from the strain data it can be inferred that this value is enlarged in about 30–40% greater than the original one. Consequently, the restored shape of the intrusion seems to be a subhorizontal lens with approximately 10 km diameter and a little less than 2 km thickness.

7. Emplacement of the Cardenchosa pluton

Investigation of the emplacement of plutons always raises the question of how room is made for the intrusion. Among the several mechanisms proposed for pluton emplacement, some can be reasonably ruled out in the case of the Cardenchosa pluton. As for stoping, it must be stressed that in this pluton enclaves are scarce, especially the xenoliths recognizable as coming from the country rocks. It is not arguable that an important quantity of xenoliths could have been mechanically disaggregated and chemically assimilated (Clarke et al., 1998), because the Cardenchosa pluton is petrographically homogeneous and the leucocratic facies of the chilled margin has no explanation in terms of assimilation. These pieces of evidence enable us to discard stoping as a significant process for making room. Regarding fault-related emplacement, faults surrounding the pluton (Fig. 1b) do not have suitable orientation and kinematics to create a potential void to be filled with granite. Finally, the tabular shape argues against ballooning.

A key issue for envisaging the intrusion mechanism of the Cardenchosa pluton is its thin tabular shape. The location of the Cardenchosa pluton just at the boundary between the Azuaga and the Sierra Albarrana units (Fig. 1b) does not seem to be coincidental. Interestingly, experimental investigations demonstrate the importance of subhorizontal rheological discontinuities for trapping the magma and forming tabular intrusions (Román-Berdiel et al., 1995a, 1997). Such a shape does not entail an important space problem, since the emplacement must have resulted from a

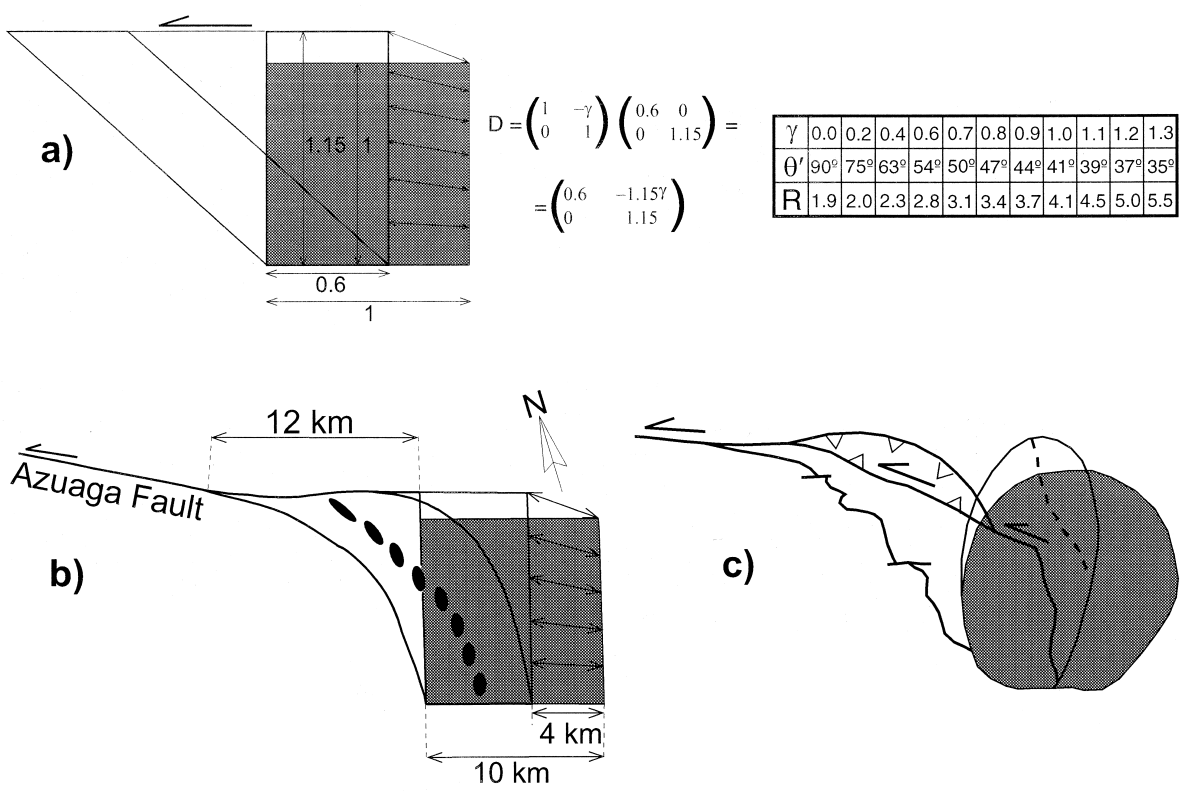

Fig. 10. (a) Deformation model consisting of a homogeneous pure shear plus a heterogeneous simple shear. Numbers in deformation matrix are shortening and stretching values inferred from strain data. The table gives the orientation, θ, and the axial ratios, R, corresponding to different values of shear strain, γ. (b) Geometry of the deformation model: the grey square is transformed first by pure shear (rectangle) and then by simple shear. (c) A more realistic expression of the shape transformation undergone by the Cardenchosa pluton. See text for more explanation.

combination of horizontal sill propagation plus roof lifting or floor depression (Cruden, 1998). The bottom of the Cardenchosa pluton is at present flat, thus making it reasonable to assume that the geometry of the intrusion was most probably laccolithic. This geometry is also indirectly supported by the extension that, associated with the low-angle normal Casa del Café fault (Figs. 1b and 11), took place just above the pluton, suggesting that the room for the pluton was made principally by roof lifting. No radiometric age is available for the Cardenchosa pluton, but the geological reasoning suggests that it intruded in Early Carboniferous times. The age of the Casa del Café fault is Late Tournaisian, which is the age of the sediments in the related Valdeinfierno basin (Wagner et al., 1983), and therefore the intrusion of the Cardenchosa pluton may well have taken place in Late Tournaisian times. This period is characterized by extensional (transtensional) tectonics all over the southwestern Iberian Massif as indicated by widespread basin generation and associated bimodal magmatism (Quesada et al., 1990). In this context, we interpret that the Cardenchosa pluton intruded in a rheological discontinuity extending laterally and upward favoured by the extensional collapse in the overburden rocks due to the Casa del Café fault (Fig. 11b).

The diameter (about 10 km) and thickness (a little less than 2 km), which result from the restoration of the Cardenchosa pluton to its intrusive shape, fit well with the (still poorly defined) empirical power law suggested by McCaffrey and Petford (1997) for the relationship between thickness and diameter of granitic intrusions. Diameter, thickness and the maximum estimated overburden of about 5–6 km are also roughly in agreement with the analogue modelling of Román-Berdiel et al. (1995a): in these experiments a thickness of about 1.5 km and a diameter of about 12.5 km correlate with an overburden of 4 km. From the reviews by Corry (1988) and Cruden (1998), it seems that the documented examples of laccolithic intrusions have paleodepths < 3 km, deeper tabular intrusions being lopolithic. The Cardenchosa pluton is perhaps a laccolithic body deeper than 3 km, although unfortunately the exact depth of intrusion cannot be definitely established due to the uncertainties on the overburden estimates from the contact aureole mineral assemblages.

The flat bottom of the Cardenchosa pluton, without any detectable root, suggests that we are not dealing with a diapir trapped in a rheological discontinuity (Brun and Pons, 1981). On the contrary, the feeding of the laccolith could have been done by dikes, which can escape detection in a gravity survey. The Early Car-

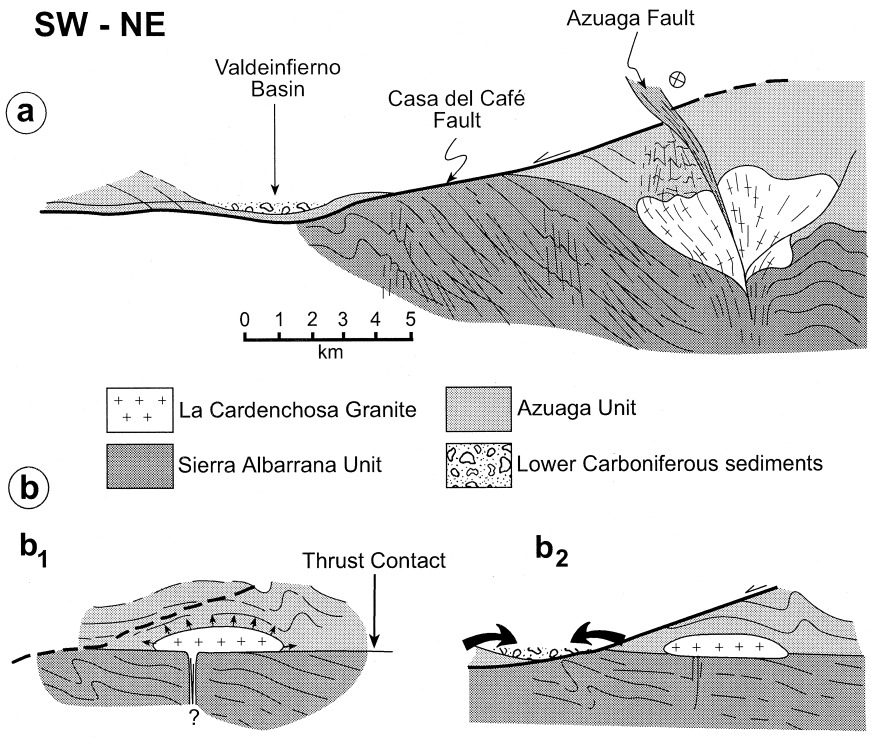

Fig. 11. (a) Geological cross-section, located in Fig. 1(b), showing the low-angle Casa del Café fault on top of the Cardenchosa pluton, and the Valdeinfierno Basin on the hanging wall of this fault. (b) Sketch showing the proposed emplacement for the Cardenchosa pluton in the contact between the Azuaga and Sierra Albarrana units; two stages are envisaged, the first one (b_1) before the movement of the Casa del Café fault (dashed line) and the second one (b_2) after the fault movement, which favoured an unloading of its footwall.

boniferous extensional stage is a tectonic scenario that easily explains the generation of fractures in the crust serving as magma conduits.

8. Conclusions

Geological mapping and gravimetric profiles have shown the tabular shape with a flat bottom and without the root of the Cardenchosa pluton. The present shape is however notably different from the one at the moment of intrusion, because the pluton has undergone solid-state deformation. The strain analysis has allowed us (a) to establish quantitatively that the pluton accommodates the kilometre-scale displacement of an important left-lateral, strike-slip fault which terminates in the pluton, and (b) to reconstruct approximately the intrusive shape of the pluton, which results in a tabular body of about 10 km diameter and a little less than 2 km thickness.

The Cardenchosa pluton intruded just at the boundary between two units of contrasting metamorphic grade. This rheological boundary seems to have conditioned the emplacement of the magma as a tabular body. More specifically, a laccolithic rather than lopolithic shape is suggested by the flat geometry of the bottom and by the extension that affected the country rocks just above the top of the intrusion, thus allowing roof lifting to occur. The intrusion is envisaged as a single pulse of magma trapped in a rheological discontinuity of the upper crust during an Early Carboniferous extensional episode. The magma can then be said to ascend through dikes (since no root has been detected) and expand laterally and upward.

This study provides additional support to the hypothesis that the majority of small to medium-sized plutons have tabular geometries and do not pose an important space problem.

Acknowledgements

We thank Francisco Gonzálvez García for improving our English text. Reviews and comments by Ken McCaffrey and Scott Paterson are appreciated. Financial support was given by the CYCIT project PB-96-1452-C03-01.

References

Ameglio, L., Vigneresse, J.L., Bouchez, J.L., 1997. Granite pluton geometry and emplacement mode inferred from combined fabric and gravity data. In: Bouchez, J.L., Hutton, D.H.W., Stephens, W.E. (Eds.), Granite: From Segregation of Melt to Emplacement Fabrics. Kluwer Academic, Dordrecht, pp. 199–214.

Aranguren, A., Larrea, F.J., Carracedo, M., Cuevas, J., Tubía, J.M., 1997. The Los Pedroches batholith (Southern Spain): polyphase interplay between shear zones in transtension and setting of granites. In: Bouchez, J.L., Hutton, D.H.W., Stephens, W.E. (Eds.), Granite: From Segregation of Melt to Emplacement Fabrics. Kluwer Academic, Dordrecht, pp. 215–229.

Aranguren, A., Tubía, J.M., Bouchez, J.L., Vigneresse, J.L., 1996. The Guitiriz granite, Variscan belt of northern Spain: extension-controlled emplacement of magma during tectonic scape. Earth and Planetary Science Letters 139, 165–176.

Azor, A., 1994. Evolución tectonometamórfica del límite entre las Zonas Centroibérica y de Ossa-Morena (Cordillera Varisca, SO de España). Ph.D. thesis, Universidad de Granada, Spain.

Azor, A., Ballèvre, M., 1997. Low-pressure metamorphism in the Sierra Albarrana area (Variscan Belt, Iberian Massif). Journal of Petrology 38, 35–64.

Azor, A., González Lodeiro, F., Simancas, J.F., 1994. Tectonic evolution of the Boundary between the Central Iberian and Ossa-Morena Zones (Variscan Belt, SW Spain). Tectonics 13, 45–61.

Bott, M.H.T., Smithson, F.B., 1967. Gravity investigations of subsurface shape and mass distribution of granite batholiths. Geological Society of America Bulletin 78, 859–878.

Bouchez, J.L., 1997. Granite is never isotropic: an introduction to AMS studies of granitic rocks. In: Bouchez, J.L., Hutton, D.H.W., Stephens, W.E. (Eds.), Granite: From Segregation of Melt to Emplacement Fabrics. Kluwer Academic, Dordrecht, pp. 95–112.

Brisbin, W.C., Green, A.G., 1980. Gravity model of the Aulneau batholith, northwestern Ontario. Canadian Journal of Earth Science 17, 968–977.

Brun, J.P., Pons, J., 1981. Strain patterns of pluton emplacement in a crust undergoing non-coaxial deformation, Sierra Morena. Journal of Structural Geology 3, 219–229.

Campos, R.C., Plata, J.L., 1991. Gravity survey. In: Development of new multi-disciplinary techniques for mineral exploration in several areas of the western Iberian Peninsula. Publicaciones especiales del boletín geológico y minero, pp. 55–66.

Clarke, D.B., Henry, A.S., White, M.A., 1998. Exploding xenoliths and the absence of 'elephants' graveyards' in granite batholiths. Journal of Structural Geology 20, 1325–1343.

Clemens, J.D., Mawer, C.K., 1992. Granitic magma transport by fracture propagation. Tectonophysics 204, 339–360.

Corry, C.E., 1988. Laccoliths: Mechanics of emplacement and growth. Geological Society of America, Special Publication 220.

Cruden, A.R., 1998. On the emplacement of tabular granites. Journal of the Geological Society of London 155, 853–862.

Dallmeyer, R.D., Quesada, C., 1992. Cadomian vs. Variscan evolution of the Ossa-Morena Zone (SW Iberia): field and $^{40}Ar/^{39}Ar$ mineral age constraints. Tectonophysics 216, 339–364.

Dehls, J.F., Cruden, A.R., Vigneresse, J.L., 1998. Fracture control of late Archean pluton emplacement in the northern Slave Province, Canada. Journal of Structural Geology 20, 1145–1154.

Delgado Quesada, M., Garrote, A., Sánchez Carretero, R., 1985. El magmatismo de la alineación La Coronada–Villaciosa de Córdoba en su mitad oriental, Zona de Ossa-Morena. Temas Geológico Mineros, IGME, Madrid, pp. 41–64.

England, R.W., 1992. The genesis, ascent and emplacement of the Northern Arran Granite, Scotland: Implications for granitic diapirism. Geological Society of America Bulletin 104, 606–614.

Fry, N., 1979. Random point distributions and strain measurement in rocks. Tectonophysics 60, 89–105.

Gapais, D., 1989. Les Orthogneiss: Structures, mécanismes de déformation et analyse cinématique. Memoires et Documents du Centre Armoricain d'Étude Structurale des Socles, Rennes, France.

Garrote, A., 1976. Asociaciones minerales del núcleo metamórfico de Sierra Albarrana, Sierra Morena Central. Memórias e Noticias Universidade de Coimbra 82, 17–39.

Garrote, A., Sánchez Carretero, R., 1979. Granitos postcinemáticos de tendencia alcalina en Ossa-Morena: el stock de La Cardenchosa (provincia de Córdoba). Acta Geológica Hispánica 14, 90–96.

Grocott, J., Brown, M., Dallmeyer, R.D., Taylor, G.K., Treloar, P.J., 1994. Mechanisms of continental growth in extensional arcs: An example from the Andean plate-boundary zone. Geology 22, 391–394.

Guillet, P., Bouchez, J.L., Wagner, J.J., 1983. Anisotropy of magnetic susceptibility and magmatic structures in the Gurande granite massif (France). Tectonics 2, 419–429.

Guineberteau, B., Bouchez, J.L., Vigneresse, J.L., 1987. The Mortagne granite pluton (France) emplaced by pull-apart along a shear zone: Structural and gravimetric arguments and regional implication. Geological Society of America Bulletin 99, 763–770.

Guineberteau, B., Cuney, M., Carr, J.L., 1989. Structure magmatique et plastique des granites de Marche Occidentale: un couloir transformant hercynien dans le nord-ouest du Massif Central français. Comptes Rendus de l'Académie des Sciences de Paris 309, 1695–1702.

Hanson, R.B., Glazner, A.F., 1995. Thermal requirements for extensional emplacement of granitoids. Geology 23, 213–216.

Hutton, D.H.W., 1988. Igneous emplacement in a shear-zone termination: The biotite granite at Strontian, Scotland. Geological Society of America Bulletin 100, 1392–1399.

Jackson, P., Sanderson, D.J., 1992. Scaling of faults displacements from the Badajoz-Córdoba shear zone, SW Spain. Tectonophysics 210, 179–190.

Kerr, A.D., Pollard, D.D., 1998. Toward more realistic formulations for the analysis of laccoliths. Journal of Structural Geology 20, 1783–1793.

Lisle, R.J., 1977. Estimations of tectonic strain ratio from the mean shape of deformed elliptical markers. Geologie en Mijnbouw 56, 140–144.

Marsh, B.D., 1982. On the mechanics of igneous diapirism, stoping and zone melting. American Journal of Science 282, 808–855.

McCaffrey, K.J.W., Petford, N., 1997. Are granitic intrusions scale invariant? Journal of the Geological Society of London 154, 1–4.

Molyneux, S.J., Hutton, D.H.W., 1995. The Ardara Pluton, Co Donegal, NW Ireland: A Straightforward Example of a Ballooning Pluton. In: Brown, M., Piccoli, M. (Eds.), The Origin of Granites and Related Rocks. Third Hutton Symposium, Abstracts, U.S. Geological Survey Circular, p. 1129.

Okudaira, T., Takeshita, T., Hara, I., Ando, I., 1995. A new estimate of the conditions for transition from basal (a) to prism [c] slip in naturally deformed quartz. Tectonophysics 250, 31–46.

Paterson, S.R., 1994. Dike transport of granitoid magmas: Comment and Reply. Geology 22, 473.

Paterson, S.R., Fowler, T.K., 1993a. Extensional pluton-emplacement models: Do they work for large plutonic complexes? Geology 21, 781–784.

Paterson, S.R., Fowler, T.K., 1993b. Re-examining pluton emplacement processes. Journal of Structural Geology 15, 191–206.

Paterson, S.R., Fowler, T.K., Miller, R.B., 1996. Pluton emplacement in arcs: a crustal-scale exchange process. Transactions of the Royal Society of Edinburgh: Earth Sciences 87, 115–123.

Paterson, S.R., Vernon, R.H., 1995. Bursting the bubble of ballooning plutons: A return to nested diapirs emplaced by multiple processes. Geological Society of America Bulletin 107, 1356–1380.

Paterson, S.R., Vernon, R.H., Tobisch, O.T., 1989. A review of criteria for the identification of magmatic and tectonic foliations in granitoids. Journal of Structural Geology 11, 349–363.

Petford, N., 1996. Dykes or diapirs? Transactions of the Royal Society of Edinburgh: Earth Sciences 87, 105–114.

Petford, N., Lister, J.R., Kerr, R.C., 1994. The ascent of felsic magmas in dykes. Lithos 32, 161–168.

Pitcher, W.S., 1979. The nature, ascent and emplacement of granitic magmas. Journal of the Geological Society of London 136, 627–662.

Pollard, D.D., Johnson, A.M., 1973. Mechanics of growth of some laccolith intrusions in the Henry Mountains, Utah, II: bending and failure of overburden layers and sill formation. Tectonophysics 18, 311–354.

Quesada, C., Robardet, M., Gabaldón, V., 1990. Ossa-Morena Zone: Synorogenic Phase (Upper Devonian–Carboniferous–Lower Permian). In: Dallmeyer, R.D., Martínez García, E. (Eds.), Pre-Mesozoic Geology of Iberia. Springer, Berlin, pp. 273–279.

Ramsay, J.G., 1967. Folding and Fracturing of Rocks. Mcgraw-Hill, New York.

Ramsay, J.G., 1989. Emplacement kinematics of a granite diapir: the Chindamora batholith, Zimbabwe. Journal of Structural Geology 11, 191–209.

Ramsay, J.G., Huber, M.I., 1983. The Techniques of Modern Structural Geology. Vol. 1. Strain Analysis. Academic Press, London.

Román-Berdiel, T., Gapais, D., Brun, J.P., 1995a. Analogue models of laccolith formation. Journal of Structural Geology 17, 1337–1346.

Román-Berdiel, T., Pueyo-Morer, E.L., Casas-Sainz, A.M., 1995b. Granite emplacement during contemporary shortening and normal faulting: structural and magnetic study of the Veiga Massif (NW Spain). Journal of Structural Geology 12, 1689–1706.

Román-Berdiel, T., Gapais, D., Brun, J.P., 1997. Granite intrusion along strike-slip zones in experiment and nature. America Journal of Science 297, 651–678.

Rosenberg, C.L., Berger, A., Schmid, S.M., 1995. Observations from the floor of a granitoid pluton: Inferences on the driving force of final emplacement. Geology 23, 443–446.

Sanderson, D.J., Roberts, S., Mcgowan, J.A., Gumiel, P., 1991. Hercynian transpressional tectonics at the southern margin of the Central Iberian Zone, west Spain. Journal of the Geological Society of London 148, 893–898.

Simancas, J.F., 1983. Geología de la extremidad oriental de la Zona Sudportuguesa. Ph.D. thesis, Universidad de Granada, Spain.

Simancas, J.F., Azor, A., Martínez Poyatos, D., González Lodeiro, F., Caro, L., 1997. Accommodation of fault displacements by granite deformation: an example from the southwestern Iberian Massif. Comptes Rendus de l'Académie des Sciences de Paris 324, 245–252.

Tikoff, B., Teyssier, Ch., 1992. Crustal-scale, en echelon "P-shear" tensional bridges: A possible solution to the batholithic room problem. Geology 20, 927–930.

Vigneresse, J.L., 1990. Use and misuse of geophysical data to determine the shape at depth of granitic intrusions. Geological Journal 25, 249–260.

Wagner, R.H., Coquel, R., Broutin, J., 1983. Mississippian floras of the Sierra Morena, SW Spain: a progress report. In: Lemos de Sousa, M.J. (Ed.), Contributions to the Carboniferous geology and palaeontology of the Iberian Peninsula. Universidade de Porto, Porto, pp. 101–125.

Weinberg, R.F., 1996. Ascent mechanism of felsic magmas: news and views. Transactions of the Royal Society of Edinburgh: Earth Sciences 87, 95–103.

Weinberg, R.F., 1999. Mesoscale pervasive felsic magma migration: alternatives to dyking. Lithos 46, 393–410.

Weinberg, R.F., Podladchikov, Y.Y., 1995. The rise of solid-state diapirs. Journal of Structural Geology 17, 1183–1195.